Ultrasound-assisted Maillard reaction of ovalbumin/xylose: The enhancement of functional properties and its mechanism

Xuanting Liu [a,b], Qi Yang [a,b], Meng Yang [a,b], Zhiyang Du [a,b], Chen Wei [a,b], Ting Zhang [a,b], Boqun Liu [a,b], Jingbo Liu [a,b,*]

[a] *Jilin Provincial Key Laboratory of Nutrition and Functional Food, Jilin University, Changchun 130062, China*
[b] *College of Food Science and Engineering, Jilin University, Changchun 130062, China*

ABSTRACT

This study aims to optimize the ultrasound treatment conditions for enhancing the degree of glycation (DG) of ovalbumin (OVA)-xylose conjugates through Maillard reaction and investigate the correlation between DG and functional properties affected by structural changes. The structural and functional properties of classical heating OVA, glycated OVA, ultrasonic treated OVA, and ultrasound-assisted glycated OVA were investigated to explore the interaction mechanism of ultrasound treatment on foaming and emulsifying properties improvement. Results indicated that the ultrasound assistance increased free sulfhydryl content, surface hydrophobicity and particle size of OVA-xylose conjugates, and thus enhancing the surface properties, which were strongly linear correlated with DG under different glycation parameters (pH, xylose/OVA ratio, heating time). Additionally, circular dichroism spectroscopy analysis revealed that ultrasound promoted the conversion of α-helices to β-sheets and unfolded structures, which was consistent with the formation of short amyloid-like aggregates that observed by atomic force microscopy phenomenon. Overall, our study provides new insights into the effects of ultrasound treatment on Maillard-induced protein functional properties enhancement, which may be a new strategy to tune the DG and functionality of protein-saccharide grafts during ultrasound processing.

1. Introduction

Egg white protein, as a functional, nutritional, and well-obtained ingredients, is widely utilized in the formulation of foods and beverages[1]. Ovalbumin (OVA), is the main protein produced from separation of value-added component present in egg white, similar to other surface-active agents, contains both hydrophilic and hydrophobic groups which have excellent foaming (air–water interface), emulsifying (water–oil interface) and gelation properties. However, the functional properties are sensitive to environmental changes (e.g. pH, ionic strength, and heating treatment)[2]. Several physical, chemical, and biochemical attempts, including irradiation[3], sonication[4], high-pressure[5], phosphorylation[6] and glycosylation[7] have been made to improve protein functional properties. Nevertheless, the physical techniques would increase processing costs, while the chemical techniques process is difficult to control and remove the remaining chemicals. Hence, developing a cost-effective and novel method to enhance

the functional properties of proteins and further broad their application in foods industry with desired functionalities is urgently needed.

Accordingly, protein-saccharide grafts are useful as a new functional biopolymer, which have excellent emulsifying[6], foaming[7], solubility[8], and heat stability[9] for food processing applications. That was due to Maillard reaction could cause more groups and regions inside the molecule to expose or induce unfolding of protein which might affect the tertiary conformation, spatial structure, and surface properties[10]. Assuredly, long processing time and higher saccharide concentration would cause higher degree of glycation (DG), with which the conformational changes would be more significant. However, the relationship between DG and functional properties improvement remains not fully clear yet. Additionally, the grafting of protein-saccharide through the Maillard reaction is a time-consuming process using dry- or wet-heating alone, which usually takes tens of hours to several weeks[11]. Moreover, the reaction extent is uncontrollable, and proteins are easily getting denaturation and aggregation at high temperatures and/or long

processing time which may have negative effects on the functionalities of the conjugates[12]. In past decades, xylose has been studied as a sugar substitute in the food, beverage, and pharmaceutical industries. Additionally, xylose could conjugate with protein and accelerate the cross-linking process which led to a higher glycation rate[13]. Fu et al.[7] found ultrasound-assisted glycation with xylose could enhance solubility and foaming properties of OVA, however, the relationship between DG and the structural and functional properties improvement of glycated proteins remains unknown. Hence, it is indispensable to looking for a more rapid and effective approach to protein structural and functional modification.

Studies have found that the Maillard reaction assisted by ultrasound treatment as an alternative strategy would be a suitable candidate for promoting the glycation of proteins with saccharide and the functional properties of grafted products can be significantly improved, which is conducive to the industrial application of the Maillard reaction. Several studies showed a number of Maillard reaction product contribute to increased antioxidative[14] and antimicrobial capacities[15], as well as high-value nutritional and functional properties (solubility, emulsifying, gelling and foaming abilities, etc.) of products that can be generated with assistance of ultrasound treatment[11]. This can be explained with the fact that ultrasound treatment could cause large number of cavitation bubbles which leads to protein unfolding and peptide bonds braking. Simultaneously, ultrasound treatment resulted in the collision probability increased between the reactive groups, speeding up the conjugation process[16]. Consequently, the grafting between protein and saccharide through the Maillard reaction was markedly accelerated and enhanced in terms of DG.

In this work, the changes in the physical and conformational changes of classical heating OVA, glycated OVA (G-OVA), ultrasonic treated OVA (U-OVA) and ultrasound-assisted glycated OVA (U-G-OVA) were investigated. The objectives of this work were to explore the interaction mechanism of ultrasound treatment on surface (foaming and emulsifying) properties improvement, and to discern the correlation between DG and functional properties of OVA. Our study would provide an attempt to improve the functional properties of OVA and expand its applications as functional agents in the food industry.

2. Materials and methods

2.1. Materials and reagents

OVA with an average molecular mass of 44.5 kDa and xylose were purchased from Sigma Chemical Co. (St. Louis, MO, USA). Other reagents were obtained from Sinopharm Chemical Reagent Co., Ltd. (Shanghai, China). All the reagents were analytical grade purity.

2.2. Preparation of the OVA-xylose conjugates

OVA (1 mg/mL) and xylose were dissolved in 50 mL phosphate buffer solution (pH 7.0) with mass ratio of 3:1, 2:1, 1:1, 1:2, 1:3. The pH of the mixtures was adjusted to 4.0, 6.0, 7.0, 8.0, 10.0 by adding 0.1 mol/L HCl and NaOH. Then, the solution was stirred for 10, 30, 60 and 120 min at 50 ℃. The browning intensity, DG, emulsifying and foaming properties of different samples were studied.

7Further, the ultrasound-assisted OVA (1 mg/mL) were dissolved in 50 mL phosphate buffer solution (pH 7.0) with xylose at mass ratio of 1:3, the pH value was adjusted to 7. The mixture was treated by the optimal ultrasound process for 61.2 min using an ultrasonic unit (20–25 kHz, JY92-2D, SCIENTZ, China) equipped with a 13 mm titanium tip probe. The sonication condition was set to an ultrasonic power of 189.5 W with pulse mode (2 s on and 5 s off) at 54 ℃. All the samples were placed in the ice bath for 30 min to stop the reaction. The surface properties and conformational changes of OVA, G-OVA, U-OVA and U-G-OVA were investigated. All the experiments were performed in triplicate.

2.3. Measurement of browning intensity

The browning intensity of the conjugate was measured according the method described by Ashoor[17] with a slight modification. In short, the samples were diluted 5-fold with 10% (w/v) sodium dodecyl sulfate (SDS) solution and 0.05 mol/L borax to a concentration of 0.2% w/v of protein. The blank samples were diluted to 1% (w/v) with deionized water. The extent of browning was measured at 420 nm (A420) by a UV–Vis spectrophotometer (UV-2550, Shimadzu, Tokyo, Japan).

2.4. Degree of glycation (DG)

The DG value of the samples were determined using the o-phthaldialdehyde (OPA) assay[18] with some modifications. OPA of 40 mg was dissolved in 1 mL of methanol, 2.5 mL of 20% (w/w) SDS and 25 mL of 0.1 mol/L borax and then adding 0.1 mL of 2-mercaptoethanol (2-ME) and finally diluted to 50 mL with distilled water. Then, 0.2 mL of sample solution was mixed with 4 mL of OPA reagent and incubated at 35 ℃ for 2 min. The mixture of distilled water and OPA reagent was used as blank. The absorbance was measured at 340 nm by a UV–Vis spectrophotometer (UV-2550, Shimadzu, Tokyo, Japan). Lysine was used as a standard to calculate the content of free amino groups. The DG value was determined as:

$$DG(\%) = \frac{A_0 - A_1}{A_0} \times 100\%$$

where A_0 and A_1 are the absorbance values before and after OVA glycated with xylose, respectively.

2.5. Emulsifying properties analysis

The emulsifying activity index (EAI) and emulsifying stability index (ESI) were determined by the turbidimetric method of Pearce and Kinsella[19]. For emulsion formation, 20 μL of 1% (w/v) protein solutions in 5 mL PBS (0.01 M, pH 7.2) and 5 mL of soybean oil were homogenized in Ultra-Turrax T25 homogenizer (AE300L-H; Shanghai Angni Instruments Co., Shanghai, China) for 2 min at 10000 rpm. After homogenization for 0 min and 10 min, 1000 μL of the emulsion was immediately taken from the bottom of the beaker, and diluted (1:100, v/v) in 0.1% (w/v) SDS solution. The absorbance was recorded at 500 nm with a UV–Vis spectrophotometer (UV-2550, Shimadzu, Tokyo, Japan). EAI and ESI were calculated as follows:

$$EAI\left(m^2g^{-1}\right) = \frac{2 \times 2.303 \times A_0 \times DF}{10^4 \times \varphi LC}$$

$$ESI(min) = \frac{10 \times A_0}{A_0 - A_{10}}$$

where DF is the dilution factor (1 0 0), C is the protein concentration (g/mL), φ is the optical path (1 cm) and is the oil phase (0.25), A_0 and A_{10} are the absorbance of the emulsion at 0 min and 10 min, respectively. Measurements were performed in triplicate.

2.6. Foaming properties analysis

The measurement of foaming properties was performed according to the modified method of Sheng et al.[20]. Briefly, an aliquot (30 mL) of 1% sample solution (w/v) was placed in a graduated glass cylinder (internal diameter 22 mm) in a water bath at 25 ℃ and whipped for 3 min with a laboratory homogenizer at a speed of 10000 rpm (AE300L-H; Shanghai Angni Instruments Co., Shanghai, China). After whipping, the propeller was immediately removed, and the glass cylinder sealed with parafilm to avoid the foam disruption. The foaming ability (FA) and foaming stability (FS) were calculated according to the following equations:

$$FA(\%) = \frac{H_0}{H_1} \times 100\%$$

$$FS(\%) = \frac{H_{30}}{H_0} \times 100\%$$

where H_1 is the foam height at before homogenizing, H_0 and H_{30} is the foam height at 0 min and 30 min after homogenizing.

2.7. Atomic force microscopy (AFM)

AFM image was generated according to the method described by Liu et al. [21] using multimode microscope (Bruker Multimode 8, Bruker (Beijing) Technology Co. Ltd, Beijing) with some modifications. The morphological properties of OVA, U-OVA, G-OVA and U-G-OVA were observed. A 5 μL supernatant was deposited on the fresh mica sheet, which was placed in sterilized clean bench to evaporate liquid. The AFM data were analyzed with the aid of NanoScope Analysis Software.

2.8. Dynamic light scattering (DLS)

The aggregation of OVA, U-OVA, G-OVA and U-G-OVA and their particle size distributions were measured by a Zetasizer Nano ZS90 particle size analyzer (Malvern, U.K.)[9]. The samples were dissolved with distilled water (0.1 mg/mL). Then 1 mL of each of the diluted samples was transferred into the measuring cell (10 mm × 10 mm × 45 mm). Subsequently, the cells were stabilized at 25 °C for 5 s and each of the measurements were obtained in triplicates at 25 °C.

2.9. Circular dichroism (CD) measurements

The CD spectra were obtained using a MOS-500 Circular Dichroism Spectrometer (Bio-Logic Science Instruments, Grenoble, France) according to the method of Greenfield[22] with some modifications. 350 μL sample solutions (0.1 mg/mL) were placed in quartz cuvettes with 0.1 cm path lengths. The measurements were recorded from 200 nm to 250 nm with a resolution of 1 nm. The structure content of α-helices, β-sheets, β-turns and unordered regions were calculated using the BeStSel software[23], which can be accessed online at http://bestsel.elte.hu.

2.10. Fourier transform infrared spectroscopy (FT-IR)

The FT-IR spectra were recorded on an IR Prestige-21 Fourier transform infrared spectrophotometer (Shimadzu, Japan)[24]. Approximately 200 mg of KBr, which was dried at 150 °C for 6 h, was mixed with 2 mg of protein sample and then pressed into a pellet under an incandescent lamp. The KBr flake was used to obtain the background spectrum. The infrared radiation absorbency scans were analyzed in the range of 4000 to 400 cm^{-1} to identify the main functional groups.

2.11. Measurement of free sulfhydryl (-SH) group

The free sulfhydryl (-SH) group contents of OVA, U-OVA, G-OVA and U-G-OVA were determined according to the method described by Beveridge, Toma and Nakai [25] with some modifications. The free -SH group was determined as follows: Ellman's reagent was prepared by dissolving 4 mg 5, 5-dithio-bis 2-nitrobenzoic acid (DTNB) (Sigma-Aldrich, Italy) in 1 mL Tris-glycine-SDS buffer (0.1 M Tris, 0.1 M glycine, 4 mM EDTA, 0.5% SDS (w/v), pH 8.0). Different treated samples (10 mg), dissolved in 5 mL Tris-glycine-SDS buffer with PBS buffer was added to the Ellman's reagent (40 μL), and the mixture was set in dark at room temperature (25 °C) for 30 min. The mixture solutions were analyzed for total and free thiol groups at a wavelength of 412 nm by a UV–vis spectrophotometer (UV-2550, Shimadzu, Tokyo, Japan) to calculate the free -SH group (As_1) as following Eq. (1):

$$Free\ SH(\mu mol/g) = 73.53 * As_1 * D/C \tag{1}$$

where As_1 in Eq. (1), is the absorbance at 412 nm, C is the sample concentration (mg solid/mL) and D is the dilution factor. The results shown are the mean values of three independent measurements.

2.12. Surface hydrophobicity (H_0) measurement

Surface hydrophobicity was determined using 1-anilino-8-naphthalenesulfonate (ANS) as a fluorescence probe according to the method of Shigeru and Shuryo [26] with some modifications. Briefly, 4 mL samples (0.5 mg/mL) were well-mixed with 20 μL 8 mM ANS solution (100 mM phosphate buffer, pH 7.0), and then incubated for 15 min at room temperature in the dark. The ANS fluorescence was excited at a wavelength of 390 nm, and the emission spectrum was collected from 400 to 600 nm by an Rf-5301pc fluorescence spectrophotometer (Shimadzu, Japan). Both slit widths used were 2 nm. The fluorescence intensity was labelled as normalized intensity (a.u.), which indicated the surface hydrophobicity. Each emission spectrum represents the average of three scans.

2.13. Experimental design and Statistical analysis

The effects of ultrasound power (50, 100, 150, 200 and 250 W), ultrasound time (0, 10, 30, 60 and 120 min) (pulse duration: on-time, 2 s; off-time, 5 s)and ultrasound temperature (50, 60, 70, 80 and 90 ℃) on DG were studied. Thereafter, the slurry was cooled in the ice-water to stop the reaction. Then, several levels with a considerable effect on the DG value were selected in accordance with the single-factor test. The Response Surface Methodology (RSM) and Box-Behnken design (BBD) method were performed to optimize the effects of ultrasound power (A), ultrasound time (B) and ultrasound temperature (C) for enhancing the DG value (Y). Encoding of factor levels is shown in Table 1. The results were analyzed by Design Expert Version 8.05 software.

All experiments were performed in triplicate and data are expressed as mean ± standard deviation (SD). Statistical analysis was performed using Least-significant difference (LSD) and regression analysis. Significant differences were determined with 95% confidence intervals.

3. Results and discussion

3.1. Effect of process parameters on DG and functional properties

The DG value and browning value of xylose-induced OVA glycation were demonstrated by different process parameters (pH, Xylose/OVA, and heating time), as shown in Fig. 1 (a-c). The browning value and DG increased first and then decreased at initial pH values ranging from 4.0 to 10.0 (Fig. 1(a)), the highest DG (27.21 ± 0.39%) was observed at pH 7.0, which might cause by the degradation of reducing sugars under non-neutral conditions[27]. Additionally, with the reducing sugar/protein ratio decreasing from 3:1 to 1:3, the DG and browning value shown the similar changing trends, which decreased sharply and then increased slightly (Fig. 1(b)). Conversely, the DG value increased with the heating time increased gradually from 0 to 120 min (Fig. 1(c)). These results potentially indicated that proteins in general can readily obtained higher DG, under conditions of high reducing sugar concentration

Table 1
The factors and levels of the Box-Behnken design for ultrasound-assisted degree of glycation of ovalbumin-xylose conjugates.

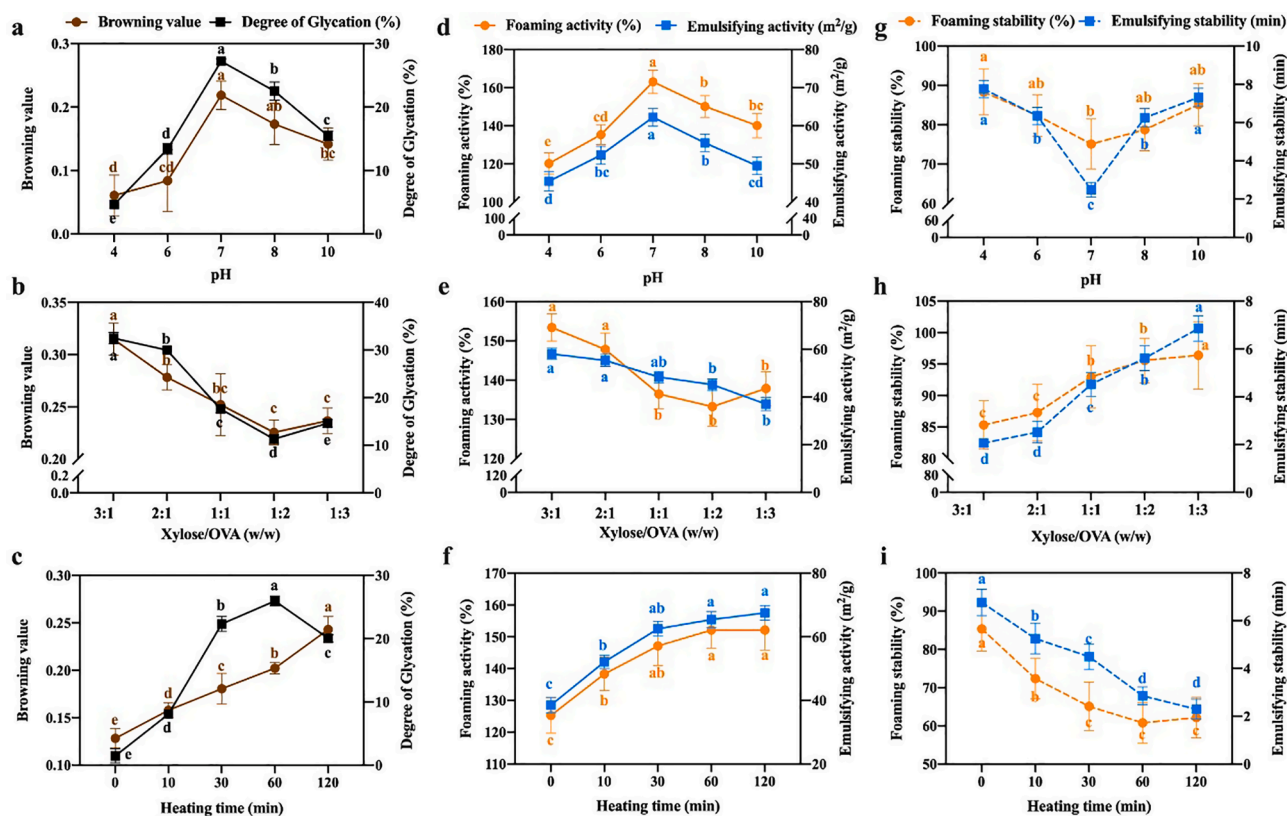| Factors	Code	Levels		
		−1	0	1
A: Ultrasound power (W)	A	150	200	250
B: Ultrasound time (min)	B	30	60	120
C: Ultrasound temperature (℃)	C	30	50	70

Fig. 1. Effect of pH, xylose/ovalbumin (OVA) ratio and heating time on browning value and degree of glycation (a-c), foaming and emulsifying activity (d-f), and foaming and emulsifying stability (g-i). Values that do not bear the same letter are significantly different ($P < 0.05$), and error bars represent the standard deviations.

and a long time heating treatment[28].

It has been widely reported that protein-saccharide grafts having excellent functional properties as a new functional biopolymer, here we investigated the effects of glycation process parameters on the emulsifying and foaming properties, consequently. The EAI (the blue line) and FA (the tangerine line) of xylose-OVA conjugates are shown in Fig. 1(d-f). A significant increase ($P < 0.05$) was found which EAI of 62.25 $\pm$ 2.33 m^2/g at pH 7, and FA was 163.12 $\pm$ 6.16% likewise. Interestingly, a similar tendency was observed for functional properties at different the sugar/protein ratio (Fig. 1(e)) and heating time (Fig. 1(f)) compared with DG. The best treatment was with 3:1 of xylose/OVA ratio, obtaining a maximum EAI of 58.10 $\pm$ 2.37 m^2/g and FA of 153.40 $\pm$ 3.49%, respectively. On the other hand, the EAI and FA increased from 38.53 $\pm$ 2.42 m^2/g to 67.52 $\pm$ 2.28 m^2/g and 125.26 $\pm$ 5.57% to 152.13 $\pm$ 6.38% with heating time ranging from 0 min to 120 min. The improvement in emulsifying and foaming performances of OVA seemed to be attributed to the increase of DG and conformational changes, which made the protein flexible and loose to increase the solubility of proteins and accelerated adsorption at the gas–water/oil–water interface. Several studies have noted that the protein-saccharide conjugates colligated the two characteristic properties of protein and saccharides often exhibit favorable emulsifying and foaming property[29–31]. Conversely, it was obvious that ESI and FS of the conjugates decreased to the minimum 2.49 $\pm$ 0.38 min and 75.12 $\pm$ 6.35% at pH 7 (Fig. 1(g)). As shown in Fig. 1(h), with the increase of saccharide-protein ratio, the ESI and FS of the conjugates significantly increased from 2.06 $\pm$ 0.03 min to 6.85 $\pm$ 0.53 min and 85.32 $\pm$ 3.87% to 96.53%, respectively. Fig. 1(i) shows the ESI and FS of influenced by heating time of glycation, the ESI and FS gradually decreased compared to the stability of the early stage of reaction. Admittedly, numerous studies have reported that proteins and polysaccharides are capable of forming associations through covalent bonds and non-covalent interactions, which allow polysaccharide-protein complexes to alter the interfacial behavior, and consequently

stabilize the emulsions[32]. However, the correlation between ESI, FS and DG value remains unclear. We assumed the probably occurred because, the unpolar compounds formed in the final stage of the Maillard reaction which caused the aggregation of denatured protein.

To further investigate the correlation between DG and functional properties, the relationship analysis was performed in Fig. 2. The correlation coefficients of DG with EA, ESI, FA and FS were depended on the glycation parameters. Noteworthy, most of the coefficients (R^2) were higher than 0.9, which indicating a strong correlation between the DG and surface properties. The correlation coefficients of EAI, ESI and DG with different processing parameters were strong positive correlation and moderate negative correlation (Fig. 2(a-b)). Similarly, the correlation between foaming properties and DG were strong ($R^2 > 0.9$) (Fig. 2 (c-d)). This indicated that glycation changed the conformational characteristics, which result in the conjugates structure unfolded and flexible and could easily expand and quickly be adsorbed at oil–water/air–water interface. With higher DG, the hydrophobicity-hydrophilicity balance would be destroyed, and thus induced the steric hindrance and hydrophilicity of the conjugates increasing, which result in the conjugates molecules more surface active and absorb to the oil phase more quickly [33]. These results inspired us to find an efficient way to enhance DG, hence ameliorate the functional properties of the conjugates.

3.2. Optimization of ultrasound treatment parameters on the DG value

As shown in Fig. 3(a-c), the browning value and DG of ultrasound-assisted glycation were demonstrated by different ultrasound power, time and temperature. With the increase of ultrasound power, the highest DG value was obtained at 200 W and then decreased slightly. Similar results were confirmed by Resendiz-Vazquez et al.[34], which indicated the ultrasound power has positive efficient in speeding up the glycation while high ultrasound power caused the protein aggregation thus prevent reaction. Correspondingly, the DG value increased quickly
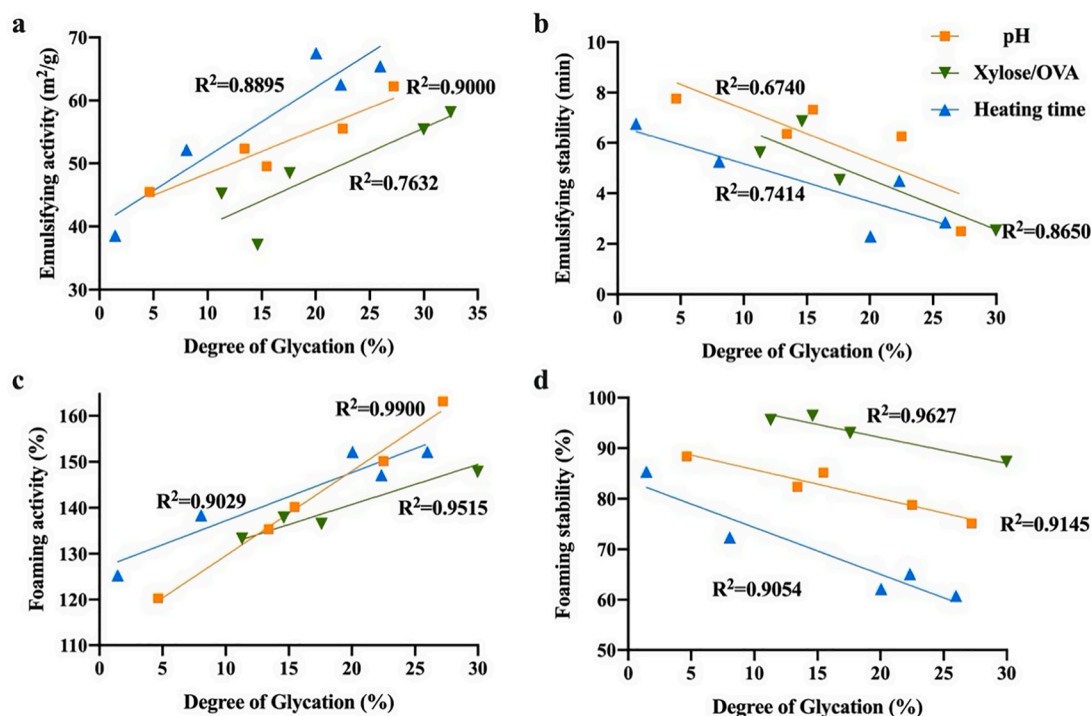
Fig.2. Correlations coefficients between degree of glycation of ovalbumin and emusifying activities (a), emusifying stability (b), foaming activities (c) and foaming stability (d).

with the rise of ultrasound time 0 to 60 min and then slight declined at 120 min, which may be caused by the aggregation of unfolded protein with flexible structure. Fig. 3(c) showed that the DG value increased at 50 to 70 °C and then decreased. According to Chen et al.[12], the extensive unfolding of protein resulting the buried reactant groups became exposed to the surface when ultrasound temperature was lower than 70 °C, however, when the temperature higher than 70 °C, protein denature and aggregation would occur, thus the DG value decreased. Hence, to optimize the ultrasound-assisted glyction parameters, the RSM experiments were performed (Fig. 3(d-i)).

The coding values of the three factors and the corresponding actual values were designed. The experimental results are shown in Table 2. The results of ANOVA are shown in Table S1. The final mathematical model can be expressed by the following quadratic equation.

$$Y = 33.89 - -0.20\,A - 0.13B + 0.95C - 0.84AB - 0.10AC + 1.25BC$$
$$- 4.36A^2 - 3.79B^2 - 2.53C^2$$

The model coefficients of determination (R^2) value for the model was 0.9850 and adjusts the complex correlation coefficient R^2 (adj) was 0.9657, which were both higher than 0.80, indicating that the model has high reliability. The quadratic regression equation obtained can predict the response value well and has a good fit. The optimal process predicted by the software involved the following conditions: ultrasound power 189.5 W, ultrasound time 61.2 min and ultrasound temperature 54 °C. In the optimal conditions, the validated experimental DG was 32.65 ± 2.34%, which matched the predicted value (33.98%) very well.

3.3. Ultrasound-assisted functional properties changes of OVA-xylose conjugates

Several studies have been proposed that glycation optimized the hydrophobic-hydrophilic balance on the protein surface, and thus modified the protein surface properties[35]. With the promotion of glycation process induced by ultrasound treatment, the surface properties of OVA, G-OVA, U-OVA and U-G-OVA were investigated as Fig. 4 showed. The conjugates were treated by ultrasound under the optimal

DG parameters according to 3.2. As expected, the foaming and emusifying activity of G-OVA increase significantly ($P < 0.05$), which might be due to the more unordered, flexible and less compact structure than native OVA. Compared with G-OVA, the U-G-OVA conjugates achieved higher FA and EAI. The results were consistent with previous results[7], reporting that the increase in functioal properties was attributed to the exposure of the internal hydrophobic groups of OVA under ultrasound treatment, which reacted easily with the reducing-end carbonyl group in polysaccharides and favored emulsion formation. The mechanical effects caused by ultrasound cavitation consequently accelerated the molecules mobility and the adsorption on the oil–water interfaces. Likewise, it can be observed that both FS and ES have been increased statistically significant ($P < 0.05$) after ultrasonication, which might be related to the balance between the aggregation and exposure of hydrophobic groups of denatured protein[36]. The increasing of surface properties susceptibility to glycation may be attributed to ultrasonic-induced conformational changes of protein, which can cause unfolding of polypeptides and exposure of buried peptide bonds, and thus make proteins more accessible for attacking. Simultaneously, ultrasound treatment resulted in the increase of collision probability between reactive groups, which could undoubtedly speeding up the conjugation process.

3.4. Macroscopic and microscopic phenomena of ultrasound-assisted glycation

The functional properties were highly correlated the protein structure, and with the physical–chemical modifications allowing greater conformational flexibility, which probably resulted in the improvement of emulsifying and foaming properties. With this consideration, we performed the AFM and DLS to investigate the ultrasound and glycation affact on macroscopic and microscopic conformational changes of OVA as shown in Fig. 5(a-d). Compared to the OVA (Fig. 5(a)), the mean particle size increased slightly from 4.17 ± 1.50 nm to 4.92 ± 1.08 nm after glycation (Fig. 5(c)). Interestingly, Fig. 5(b) show that ultrasound treatment slightly reduced the protein size and a broadening of particle
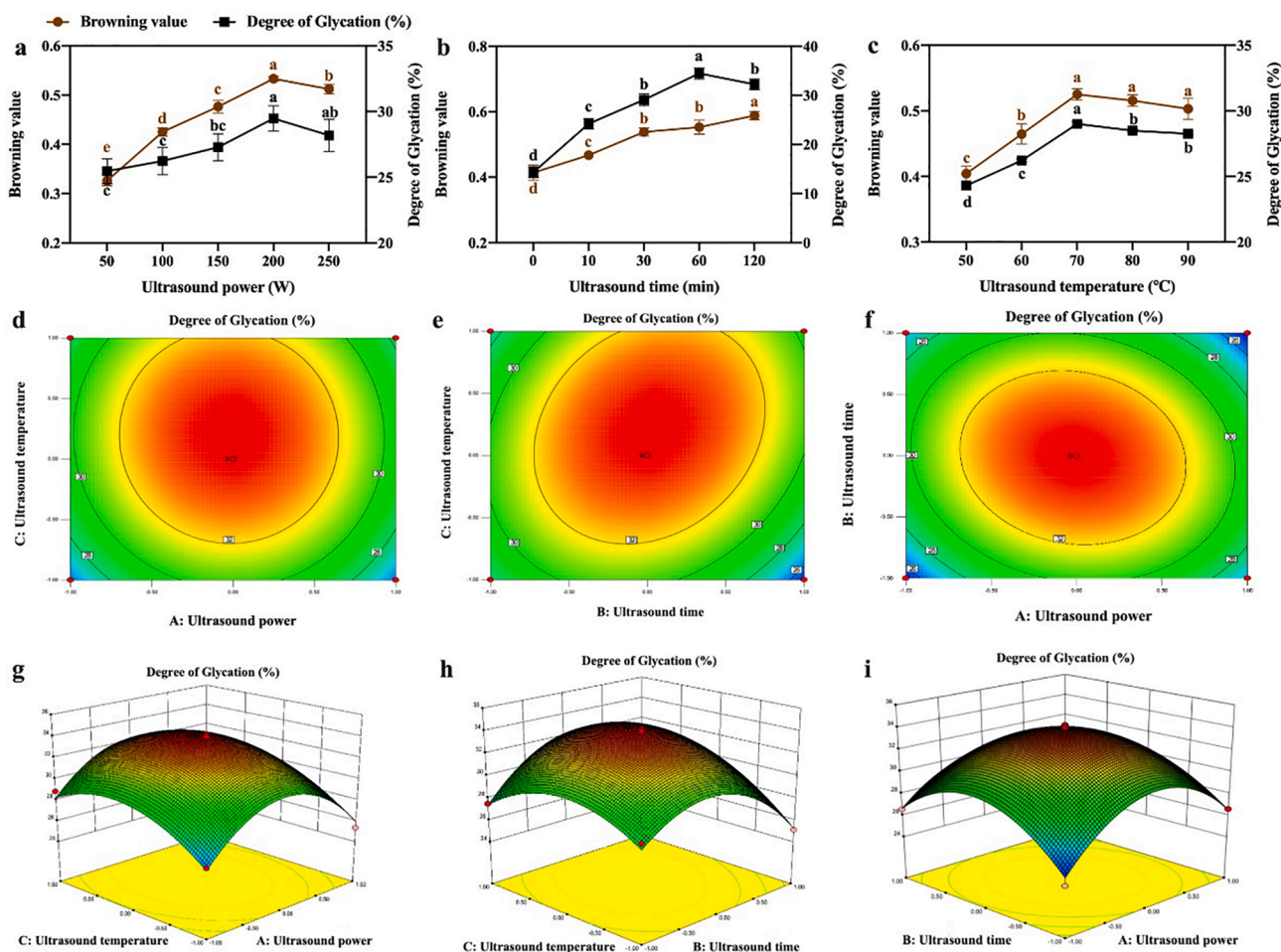
Fig. 3. Effect of ultrasond power (a), ultrasond time (b) and ultrasound temperature (c) on browing value of ovalbumin. The corresponding plots and three-dimensional plots of the three variables (A: ultrasound power; B: ultrasound time; C: ultrasound temperature) on the response (degree of glycation). Values that do not bear the same letter are significantly different (*P < 0.05*), and error bars represent the standard deviations.

size distribution, which attributed that high ultrasound energy could cause modifications in protein molecules like breaking of covalent bonds, generation of low molecular weight peptides, and/or fragmentation of large aggregates into smaller particles[37]. Moreover, the mean particle size significantly increased to 86.73 ± 6.18 nm ($P < 0.05$) with ultrasound-assisted glycation, which provides significant evidence that OVA denatures and forms aggregates. We speculated the phenomenon was due to the ultrasound treatment speeds up the Maillard reaction which resulting in higher DG, and thus promoting the rearrangement of the conjugates. Similarly, Liu et al. [9] found that high polysaccharides concentration resulted in higher DG, and thus promoted the formation of short amyloid-like aggregates.

To validate these hypotheses, the morphology and depth of OVA, U-OVA, G-OVA and U-G-OVA was investigated using AFM. Obviously, ultrasound treatment increased the depth of protein molecules as shown in Fig. 5(b) and Fig. 5(d), which might due to the hydrophobic groups and regions existed in the interior of OVA molucules were exposed to the surface. Notably, for the U-G-OVA, the AFM images revealed that the OVA has a tendency to form a fibrous structure. According to Jones & Mezzenga[38], the building blockes of amyloid-like aggregates linked by intermolecular β-sheet, and hydrophobic sequestering in the interior gap may be partly responsible for the formantion of β-sheet. A similar phenomenon was observed by Wei & Huang[39], whose speculated that the building blockes of ultrasound treated samples could linked with more saccharides and resulted in the formation of aggregation in a twisted coil way to diminish streric hindrance brought by saccharides.

According to Wang et al.[40], amyloid-like fibrils from food proteins possess unique functional properties due to the fibril structures formed stonger entanglement among the macromolecules. Overall, the macroscopic and microscopic phenomena were attributed to the conformational changes, thereby resulting in the enhancement of surface properties.

Table 2
Box-Behnken design matrix with the encoded ultrasound-assisted degree of glycation of ovalbumin-xylose conjugates.

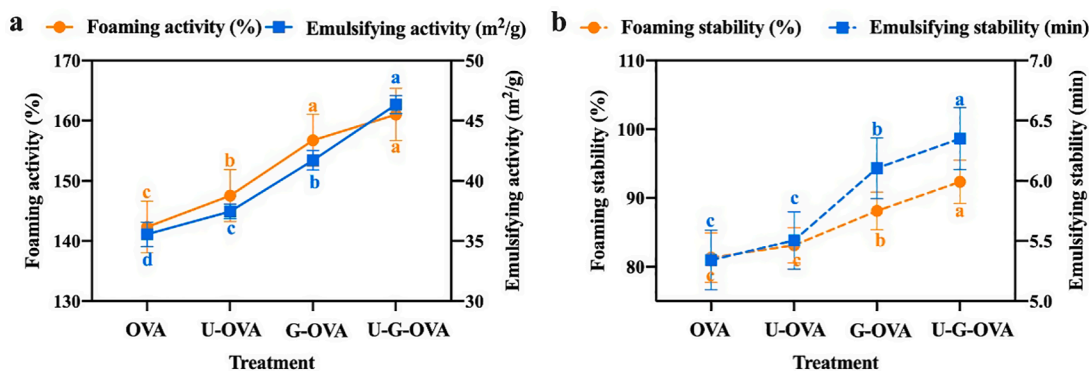| Order	A: Ultrasound power (W)	B: Ultrasound time (min)	C: Ultrasound temperature (°C)	Degree of glycation (%)
1	0	0	0	33.17 ± 0.89
2	1	1	0	25.27 ± 1.35
3	−1	−1	0	24.52 ± 1.19
4	1	0	−1	25.34 ± 0.56
5	0	1	−1	25.11 ± 2.11
6	−1	1	0	26.56 ± 1.54
7	−1	0	−1	26.35 ± 0.93
8	1	0	1	27.44 ± 0.32
9	0	−1	−1	28.52 ± 1.05
10	−1	0	1	28.85 ± 0.45
11	0	−1	1	27.51 ± 0.68
12	0	0	0	34.11 ± 1.29
13	1	−1	0	26.59 ± 2.23
14	0	0	0	34.07 ± 0.76
15	0	0	0	34.22 ± 1.39
16	0	1	1	29.12 ± 0.37
17	0	0	0	33.89 ± 1.45

Fig. 4. Foaming and emulsifying properties of classical heating ovalbumin (OVA), ultrasound-assisted OVA (U-OVA), glycated OVA (G-OVA) and ultrasound-assisted glycated OVA (U-G-OVA). (Note: ultrasound power 189.5 W, ultrasound time 61.2 min, and ultrasound temperature 54 °C). Values that do not bear the same letter are significantly different ($P < 0.05$), and error bars represent the standard deviations.
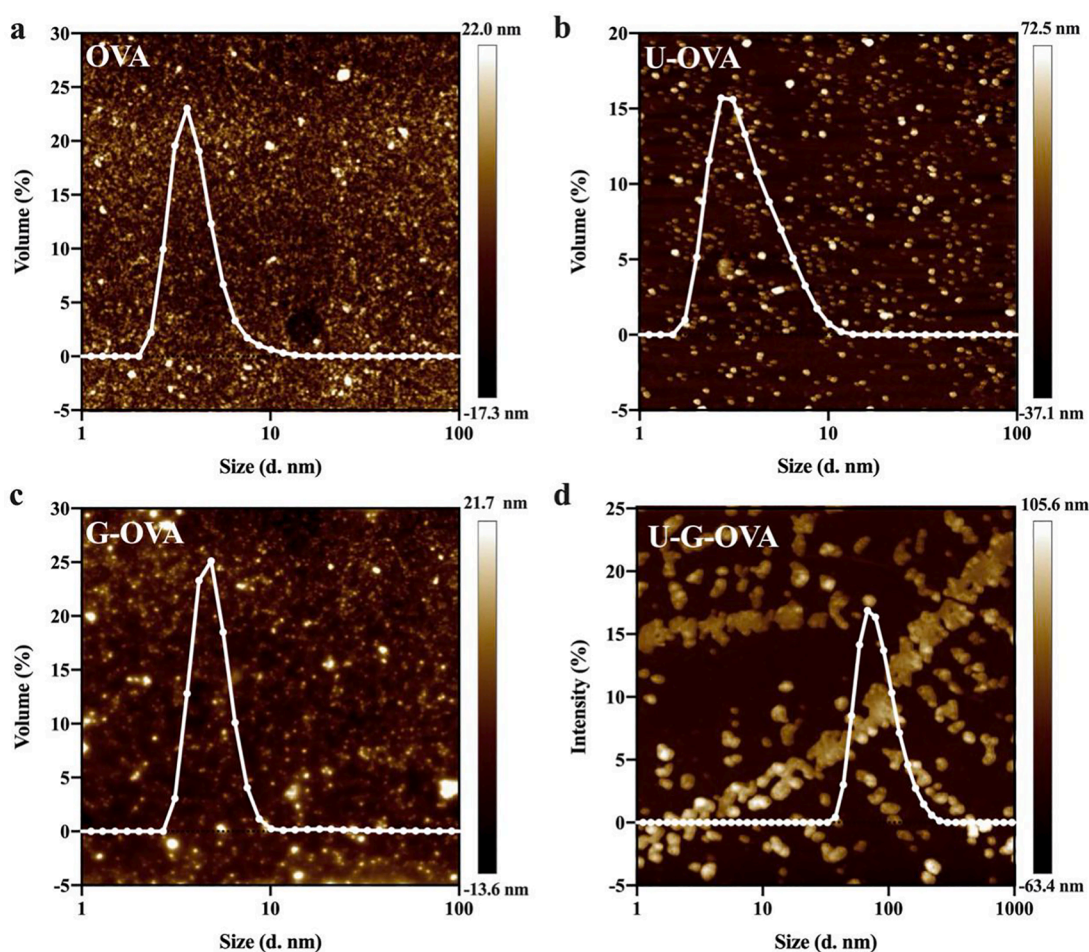

Fig. 5. Microstructure of ovalbumin (OVA) (a), ultrasound-assisted OVA (U-OVA) (b), glycated OVA (G-OVA) (c) and ultrasound-assisted glycated OVA (U-G-OVA) (d). Dynamic light scattering result is superimposed on the atomic force microscopy images with the horizontal scale showing particle size (nm). (Note: ultrasound power 189.5 W, ultrasound time 61.2 min, and ultrasound temperature 54 °C).

3.5. Secondary structure analysis

The results of secondary structure and functional groups changes performed by CD and FT-IR presented in Fig. 6 seemed to confirm further the hypothesis of ultrasonic-induced structural changes of OVA. The secondary structure content of OVA, U-OVA, G-OVA and U-G-OVA were estimated using CD secondary analysis tool BeStSel[23]. Compared with the classical heating sample (black volume), with ultrasound

treatment, the α-helix content decreased from 25.07 ± 1.815% to 19.73 ± 1.93%, while the content of unfolded structures increased significantly from 37.03 ± 1.57% to 41.10 ± 2.42% and β-sheet increased slightly from 24.43 ± 1.04% to 25.20 ± 1.21%, which indicated the ultrasound drives the conversion of α-helix to unfold structures and β-sheet. It might be due to the binding of polysaccharides to protein involves a condensation between the carbonyl group and ε-amino group, which is within the α-helix region or its neighbor protein[12,41]. With
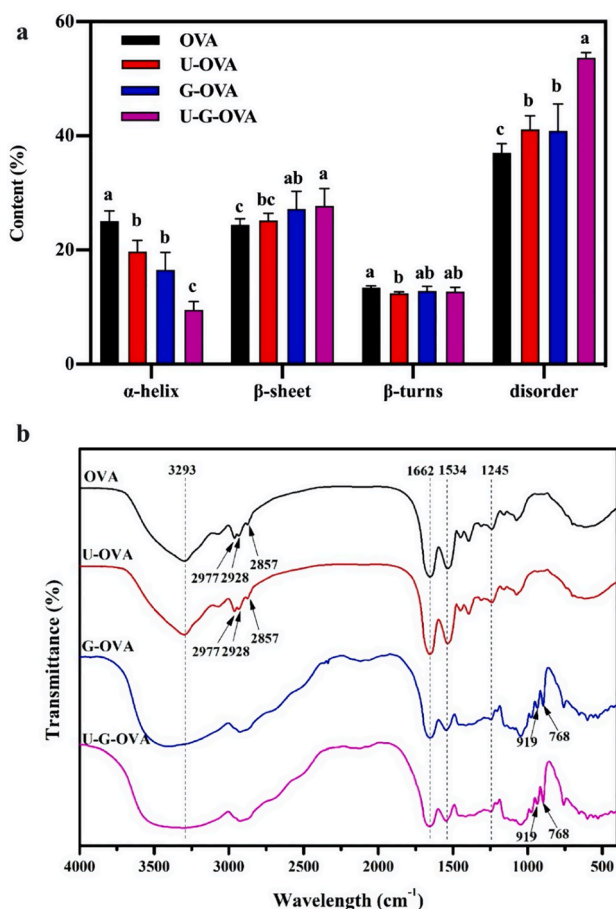
Fig. 6. Secondary structure content (a) and functional groups changes (b) of ovalbumin (OVA), ultrasound-assisted OVA (U-OVA), glycated OVA (G-OVA) and ultrasound-assisted glycated OVA (U-G-OVA). (Note: ultrasound power 189.5 W, ultrasound time 61.2 min, and ultrasound temperature 54 °C). Values that do not bear the same letter are significantly different ($P < 0.05$), and error bars represent the standard deviations.

the assistance of ultrasound treatment, more evident changes in the distribution of secondary structure were found. The observed changes may be related to the DG, and higher DG endowed lower α-helix content [42]. The decrease in α-helix ($9.53 \pm 1.43\%$) and increase in β-sheet ($27.70 \pm 3.08\%$) and unfolded structures ($53.67 \pm 0.92\%$) of U-G-OVA indicative the higher DG promoted by ultrasound, which may contribute to the improvement of surface properties. The increase in OVA's β-sheet content provides further evidence of fibrillar conformation as shown in Fig. 5(d). Analogously, several previous reports proved that ultrasound assisted glycation caused protein unfolding would give a novel of protein functional properties enhancement[12,43,44].

FT-IR spectroscopy was used to characterize the intermolecular interactions between xylose and OVA, where the results of OVA, xylose-OVA conjugates, ultrasound-assisted OVA, and ultrasound-assisted conjugates were shown in Fig. 6(b). The chemical changes in xylose-OVA conjugates would lead to the formation of functional groups, such as Amadori compound (C = O), Schiff base (C = N), and pyrazines (C-N)[45]. The typical broad band in 3200–3600 cm^{-1} region (amide A) became wide in G-OVA and U-G-OVA, which suggesting that the stretching vibration of intermolecular H-bonded N–H and O–H groups after glycation[5]. The wavenumber associated with the stretching of the C–H bonds in methyl groups (–CH$_3$) at 2857, 2928 and 2977 cm^{-1} shifted as one peak at 2977 cm^{-1} after the glycation, which indicated the xylose was successfully conjugated to OVA. The peaks signal intensity located at approximately 1662 and 1534 cm^{-1} decreased after glycation, which are attributed to amide I (C = O stretching) and amide II (N–H

deformation), respectively[33]. For G-OVA and U-G-OVA, there are a series of peaks in the 543–1050 cm^{-1} region, which could be ascribed to the vibration modes of C-O and C–C stretches and bending mode of C–H [46], especially at 768 and 919 cm^{-1}. The adsorptions of the glycation samples indicated the consumption of amine groups and the formation of covalent bond in Schiff base. Additionally, the absorptions of conjugates in 950–1050 cm^{-1} regions were stronger than those of OVA and U-OVA, which indicated the side-chain vibrations and alteration of protein structure[47], and thus probably resulting in the exposure of more hydrophobic clusters and increase the surface properties of OVA. This proved the effect of ultrasound treatment on accelerating the glycation reaction and was consistent with the results of DG, AFM and CD analysis.

3.6. Free sulfhydryl content and surface hydrophobicity analysis

To further probe the effect of ultrasonic pretreatment on Maillard-induced protein structural conformation changes, we characterized the surface exposed hydrophobic regions of proteins by ANS fluorescence, and the free sulfhydryl group (-SH) content. Fig. 7(a) show the ANS fluorescence intensity of OVA, G-OVA, U-OVA, and U-G-OVA, respectively. For the Maillard-induced samples (blue line), the intensity of the maximum peak drastically increased from 83.73 a.u. for the control samples (black line) to 131.05 a.u. after grafting with xylose, which probably demonstrated the expose of hydrophobic groups due to the protein unfolding and the saccharide modification resulted in the aggregation via crosslinking hydrophobic interactions. Although some reports proved that the conjugates hydrophobic groups buried in intramolecularly due to the bonding of hydrophilic straight-chain polysaccharide increasing the hydrophilicity on the molecule surface, thus inhibited the accessibility of ANS[12,48]. However, compared to the classical heating OVA and G-OVA, the ANS fluorescence intensity of U-G-OVA was significantly increased with ultrasound treatment, which was consistent with the hypothesis according to AFM results. We supposed the reason may because the ultrasonic cavitation and mechanical effect generated in the biopolymer solution to destroy protein conformation and structure, which leading to protein subunit dissociation and the internal hydrophobic residues exposed. This presumably promoted the Mallard reaction and resulted in the peptide chain being more unfolded and surface hydrophobicity enhancement. Analogously, Xie et al.[49] also illustrated that ultrasonic-induced saccharide modification of protein exhibited higher surface hydrophobicity than native protein.

Simultaneously, the free sulfhydryl group (-SH) content of OVA-xylose conjugates obtained by ultrasonic treatment were significantly higher than that of conjugates obtained by glycation and ultrasound treatment, respectively (Fig. 7(b)). As shown, the content of free -SH groups of OVA showed an increase with ultrasound treatment (U-OVA), which revealed the unfolding of OVA. Correspondingly, most -SH groups that exited in the interior of OVA were exposed with ultrasound denaturation[50], and thereby causing the enhancement of DG and the rearrangement of conjugates, which correlated with the improvement of foaming and emulsifying properties (Fig. 4). A similar result was reported by Chen et al.[51], who attributed that the ultrasonic cavitation effect and mechanical effect destroyed the protein conformation and structure, which resulted in the exposure of the internal hydrophobic residues and buried -SH groups. Overall, the improvement in functional performances of OVA proved to be associated with the conformational changes and was positively correlated with both free sulfhydryl content and surface hydrophobicity.

4. Conclusion

Ultrasound treatment was able to speed up the DG between OVA and xylose, which has a strong linear correlation with the surface properties. Ultrasound treatment significantly increased the DG of OVA which the optimum treatment conditions were: ultrasound power 189.5 W,
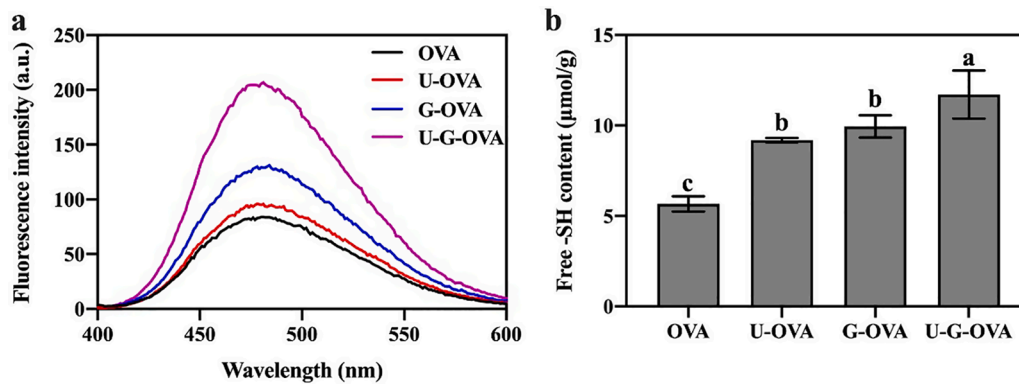
Fig. 7. Surface hydrophobicity (H_0) (a) and free sulfhydryl group (b) of ovalbumin (OVA), ultrasound-assisted OVA (U-OVA), glycated OVA (G-OVA) and ultrasound-assisted glycated OVA (U-G-OVA). (Note: ultrasound power 189.5 W, ultrasound time 61.2 min, and ultrasound temperature 54 °C). Values that do not bear the same letter are significantly different ($P < 0.05$), and error bars represent the standard deviations.

ultrasound time 61.2 min and ultrasound temperature 54 °C. The structural changes induced by ultrasound were found to mainly involve tertiary and secondary structure, in which loss of α-helix with the formation of β-sheet and disorder was presented, and causing an increase in free sulfhydryl content and surface hydrophobicity. Moreover, The ultrasound treatment induces the formation of amyloid-like fibrils structure, which helps to form a network structure of conjugates, hence result in the enhancement of surface properties. Therefore, covalent linkage of OVA with xylose through ultrasound-assisted Maillard reaction might be an ideal method to improve its functional properties and thus expand its utilization in the food industry. More investigations on the glycation mechanism between protein and polysaccharides and process optimization under ultrasound treatment need to be carried out in the future.

CRediT authorship contribution statement

Xuanting Liu: Writing - original draft, Project administration, Data curation. **Qi Yang:** Investigation, Validation, Visualization. **Meng Yang:** Validation, Data curation, Writing - review & editing. **Zhiyang Du:** Formal analysis, Visualization. **Chen Wei:** Investigation, Validation. **Ting Zhang:** Writing - review & editing. **Boqun Liu:** Methodology, Software. **Jingbo Liu:** Project administration, Resources, Supervision.

Declaration of Competing Interest

The authors declare that they have no known competing financial interests or personal relationships that could have appeared to influence the work reported in this paper.

Appendix A. Supplementary data

Supplementary data to this article can be found online at https://doi.org/10.1016/j.ultsonch.2021.105477.

References

[1] Y. Mine, Recent advances in egg protein functionality in the food system, World's Poult. Sci. J. 58 (2002) 31–39.
[2] J.M.S. Renkema, H. Gruppen, T. van Vliet, Influence of pH and ionic strength on heat-induced formation and rheological properties of soy protein gels in relation to denaturation and their protein compositions, J. Agric. Food. Chem. 50 (2002) 6064–6071.
[3] X. Liu, J. Liu, W. Zhang, S. Han, T. Zhang, B. Liu, Electron beam irradiation-induced structural changes increase the antioxidant activities of egg white protein, LWT - Food Science and Technology 111 (2019) 846–852.
[4] J. O'Sullivan, M. Arellano, R. Pichot, I. Norton, The effect of ultrasound treatment on the structural, physical and emulsifying properties of dairy proteins, Food Hydrocolloids 42 (2014) 386–396.
[5] X. Chen, R. Zhou, X. Xu, G. Zhou, D. Liu, Structural modification by high-pressure homogenization for improved functional properties of freeze-dried myofibrillar proteins powder, Food Res. Int. 100 (2017) 193–200.
[6] S. Tang, J. Yu, L. Lu, X. Fu, Z. Cai, Interfacial and enhanced emulsifying behavior of phosphorylated ovalbumin, Int. J. Biol. Macromol. 131 (2019) 293–300.
[7] X. Fu, Q. Liu, C. Tang, J. Luo, X. Wu, L. Lu, Z. Cai, Study on structural, rheological and foaming properties of ovalbumin by ultrasound-assisted glycation with xylose, Ultrason. Sonochem. 58 (2019), 104644.
[8] H. Kchaou, N. Benbettaieb, M. Jridi, M. Nasri, F. Debeaufort, Influence of Maillard reaction and temperature on functional, structure and bioactive properties of fish gelatin films, Food Hydrocolloids 97 (2019), 105196.
[9] X. Liu, J. Liu, W. Zhang, R. Pearce, M. Chen, T. Zhang, B. Liu, Effect of the degree of glycation on the stability and aggregation of bovine serum albumin, Food Hydrocolloids 106 (2020), 105892.
[10] F. Xue, Z. Wu, J. Tong, J. Zheng, C. Li, Effect of combination of high-intensity ultrasound treatment and dextran glycosylation on structural and interfacial properties of buckwheat protein isolates, Bioscience, Biotechnology, and Biochemistry 81 (2017) 1891–1898.
[11] H. Yu, Q. Zhong, Y. Liu, Y. Guo, Y. Xie, W. Zhou, W. Yao, Recent advances of ultrasound-assisted Maillard reaction, Ultrason. Sonochem. 64 (2020), 104844.
[12] W. Chen, X. Ma, W. Wang, R. Lv, M. Guo, T. Ding, X. Ye, S. Miao, D. Liu, Preparation of modified whey protein isolate with gum acacia by ultrasound maillard reaction, Food Hydrocolloids 95 (2019) 298–307.
[13] R. ter Haar, Y. Westphal, P.A. Wierenga, H.A. Schols, H. Gruppen, Cross-linking behavior and foaming properties of bovine α-Lactalbumin after glycation with various saccharides, J. Agric. Food. Chem. 59 (2011) 12460–12466.
[14] O. Abdelhedi, L. Mora, I. Jemil, F. Toldrá, M. Nasri, R. Nasri, Effect of ultrasound pretreatment and Maillard reaction on structure and antioxidant properties of ultrafiltrated smooth-hound viscera proteins-sucrose conjugates, Food Chem. 230 (2017) 507–515.
[15] H. Zhang, J. Yang, Y. Zhao, High intensity ultrasound assisted heating to improve solubility, antioxidant and antibacterial properties of chitosan-fructose Maillard reaction products, LWT - Food Science and Technology 60 (2015) 253–262.
[16] C. Zhao, H. Yin, J. Yan, X. Niu, B. Qi, J. Liu, Structure and acid-induced gelation properties of soy protein isolate–maltodextrin glycation conjugates with ultrasonic pretreatment, Food Hydrocolloids 112 (2021), 106278.
[17] S.H. Ashoor, J.B. Zent, Maillard browning of common amino acids and sugars, J. Food Sci. 49 (1984) 1206–1207.
[18] M.S. Vigo, L.S. Malec, R.G. Gomez, R.A. Llosa, Spectrophotometric assay using o-phthaldialdehyde for determination of reactive lysine in dairy products, Food Chem. 44 (1992) 363–365.
[19] K.N. Pearce, J.E. Kinsella, Emulsifying properties of proteins: evaluation of a turbidimetric technique, J. Agric. Food. Chem. 26 (1978) 716–723.
[20] L. Sheng, G. Tang, Q. Wang, J. Zou, M. Ma, X. Huang, Molecular characteristics and foaming properties of ovalbumin-pullulan conjugates through the Maillard reaction, Food Hydrocolloids 100 (2020), 105384.
[21] G. Liu, Q. Wang, Z. Hu, J. Cai, X. Qin, Maillard-reacted whey protein isolates and epigallocatechin gallate complex enhance the thermal stability of the Pickering emulsion delivery of curcumin, J. Agric. Food. Chem. 67 (2019) 5212–5220.
[22] N.J. Greenfield, Using circular dichroism spectra to estimate protein secondary structure, Nature Protocol 1 (2006) 2876–2890.
[23] A. Micsonai, F. Wien, É. Bulyáki, J. Kun, É. Moussong, Y.-H. Lee, Y. Goto, M. Réfrégiers, J. Kardos, BeStSel: a web server for accurate protein secondary structure prediction and fold recognition from the circular dichroism spectra, Nucleic Acids Res. 46 (2018) W315–W322.

[24] Z. Du, J. Liu, H. Zhang, Y. Chen, X. Wu, Y. Zhang, X. Li, T. Zhang, H. Xiao, B. Liu, l-Arginine/l-lysine functionalized chitosan–casein core–shell and pH-responsive nanoparticles: fabrication, characterization and bioavailability enhancement of hydrophobic and hydrophilic bioactive compounds, Food Funct. 11 (2020) 4638–4647.

[25] T. Beveridge, S.J. Toma, S. Nakai, Determination of SH- and SS-groups in some food proteins using Ellman's reagent, J. Food Sci. 39 (1974) 49–51.

[26] H. Shigeru, N. Shuryo, Contribution of Hydrophobicity, Net charge and sulfhydryl groups to thermal properties of ovalbumin, Canadian Institute of Food Science and Technology Journal 18 (1985) 290–295.

[27] E.H. Ajandouz, L.S. Tchiakpe, F.D. Ore, A. Benajiba, A. Puigserver, Effects of pH on caramelization and Maillard reaction kinetics in fructose-Lysine model systems, J. Food Sci. 66 (2001) 926–931.

[28] P. Sutthirak, S. Dharmsthiti, S. Lertsiri, Effect of glycation on stability and kinetic parameters of thermostable glucoamylase from Aspergillus niger, Process Biochemistry 40 (2005) 2821–2826.

[29] Q. Zhang, L. Li, Q. Lan, M. Li, D. Wu, H. Chen, Y. Liu, D. Lin, W. Qin, Z. Zhang, J. Liu, W. Yang, Protein glycosylation: a promising way to modify the functional properties and extend the application in food system, Crit. Rev. Food Sci. Nutr. 59 (2019) 2506–2533.

[30] C.M. Oliver, L.D. Melton, R.A. Stanley, Creating proteins with novel functionality via the Maillard reaction: A review, Crit. Rev. Food Sci. Nutr. 46 (2006) 337–350.

[31] F.C. de Oliveira, J.S.D.R. Coimbra, E.B. de Oliveira, A.D.G. Zuñiga, E.E.G. Rojas, Food protein-polysaccharide conjugates obtained via the Maillard reaction: A review, Crit. Rev. Food Sci. Nutr. 56 (2016) 1108–1125.

[32] E. Dickinson, Hydrocolloids at interfaces and the influence on the properties of dispersed systems, Food Hydrocolloids 17 (2003) 25–39.

[33] Y. Xu, M. Dong, C. Tang, M. Han, X. Xu, G. Zhou, Glycation-induced structural modification of myofibrillar protein and its relation to emulsifying properties, LWT - Food Science and Technology 117 (2020), 108664.

[34] J.A. Resendiz-Vazquez, J.A. Ulloa, J.E. Urías-Silvas, P.U. Bautista-Rosales, J.C. Ramírez-Ramírez, P. Rosas-Ulloa, L. González-Torres, Effect of high-intensity ultrasound on the technofunctional properties and structure of jackfruit (Artocarpus heterophyllus) seed protein isolate, Ultrason. Sonochem. 37 (2017) 436–444.

[35] A.O. Matemu, H. Kayahara, H. Murasawa, S. Nakamura, Importance of size and charge of carbohydrate chains in the preparation of functional glycoproteins with excellent emulsifying properties from tofu whey, Food Chem. 114 (2009) 1328–1334.

[36] A.C. Soria, M. Villamiel, Effect of ultrasound on the technological properties and bioactivity of food: a review, Trends Food Sci. Technol. 21 (2010) 323–331.

[37] O.L. Tavano, Protein hydrolysis using proteases: An important tool for food biotechnology, J. Mol. Catal. B Enzym. 90 (2013) 1–11.

[38] J. Adamcik, R. Mezzenga, Proteins fibrils from a polymer physics perspective, Macromolecules 45 (2012) 1137–1150.

[39] Z. Wei, Q. Huang, Modification of ovotransferrin by Maillard reaction: Consequences for structure, fibrillation and emulsifying property of fibrils, Food Hydrocolloids 97 (2019), 105186.

[40] Y. Wang, Y. Shen, G. Qi, Y. Li, X.S. Sun, D. Qiu, Y. Li, Formation and physicochemical properties of amyloid fibrils from soy protein, Int. J. Biol. Macromol. 149 (2020) 609–616.

[41] C. Li, H. Xue, Z. Chen, Q. Ding, X. Wang, Comparative studies on the physicochemical properties of peanut protein isolate–polysaccharide conjugates prepared by ultrasonic treatment or classical heating, Food Res. Int. 57 (2014) 1–7.

[42] Y. Xu, Y. Zhao, Z. Wei, H. Zhang, M. Dong, M. Huang, M. Han, X. Xu, G. Zhou, Modification of myofibrillar protein via glycation: Physicochemical characterization, rheological behavior and solubility property, Food Hydrocolloids 105 (2020), 105852.

[43] O.A. Higuera-Barraza, W. Torres-Arreola, J.M. Ezquerra-Brauer, F.J. Cinco-Moroyoqui, J.C. Rodríguez Figueroa, E. Marquez-Ríos, Effect of pulsed ultrasound on the physicochemical characteristics and emulsifying properties of squid (Dosidicus gigas) mantle proteins, Ultrason. Sonochem. 38 (2017) 829–834.

[44] L. Chen, J. Chen, K. Wu, L. Yu, Improved low pH emulsification properties of glycated peanut protein isolate by ultrasound Maillard reaction, J. Agric. Food. Chem. 64 (2016) 5531–5538.

[45] M. Nooshkam, A. Madadlou, Maillard conjugation of lactulose with potentially bioactive peptides, Food Chem. 192 (2016) 831–836.

[46] F.-L. Gu, J.M. Kim, S. Abbas, X.-M. Zhang, S.-Q. Xia, Z.-X. Chen, Structure and antioxidant activity of high molecular weight Maillard reaction products from casein–glucose, Food Chem. 120 (2010) 505–511.

[47] M.C. Chang, J. Tanaka, FT-IR study for hydroxyapatite/collagen nanocomposite cross-linked by glutaraldehyde, Biomaterials 23 (2002) 4811–4818.

[48] F. Xue, C. Li, X. Zhu, L. Wang, S. Pan, Comparative studies on the physicochemical properties of soy protein isolate-maltodextrin and soy protein isolate-gum acacia conjugate prepared through Maillard reaction, Food Res. Int. 51 (2013) 490–495.

[49] Y. Xie, J. Wang, Y. Shi, Y. Wang, L. Cheng, L. Liu, N. Wang, H. Li, D. Wu, F. Geng, Molecular aggregation and property changes of egg yolk low-density lipoprotein induced by ethanol and high-density ultrasound, Ultrasonics Sonochemistry 63 (2020), 104933.

[50] A.B. Stefanović, J.R. Jovanović, M.B. Dojčinović, S.M. Lević, V.A. Nedović, B.M. Bugarski, Z.D. Knežević-Jugović, Effect of the Controlled High-Intensity Ultrasound on improving functionality and structural changes of egg white proteins, Food Bioprocess Technol. 10 (2017) 1224–1239.

[51] J. Chen, X. Zhang, Y. Chen, X. Zhao, B. Anthony, X. Xu, Effects of different ultrasound frequencies on the structure, rheological and functional properties of myosin: Significance of quorum sensing, Ultrason. Sonochem. 69 (2020), 105268.